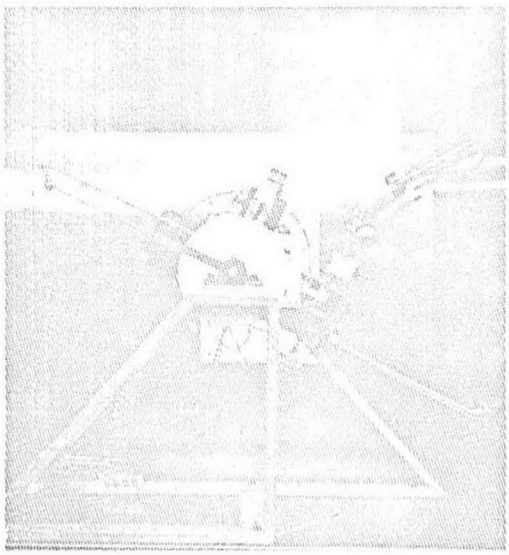

Multipurpose free-piston P-V-T and phase equilibrium test cell.

function is known. If highly accurate values of the second virial coefficient are available, new information can be obtained regarding the adequacy of the various potential functions and combining rules (*5, 6*). Although the calculations are extremely difficult for all but the simplest potential functions, the third virial can be calculated by consideration of all possible two-body interactions in the three-body system.

Extensive and very accurate *P-V-T* data are required to yield second virial values accurate to better than 1% (*7*). Accuracies considerably better than this are desirable if information is to be extracted regarding interaction coefficients for mixtures and especially if potential function parameter combining rules are to be tested (*6*). In addition to the use of least-squares fitting of data to obtain second virial values, it is often convenient to obtain values graphically by use of compressibility factor data, *i.e.*, rearrangement of the virial equation yields,

$$(Z-1)V = B + C/V + D/V^2 + \cdots \quad (7)$$

From this, the second virial may be found by plotting $(Z-1)V$ versus $1/V$ and extrapolating to the ordinate to obtain:

$$\lim_{(1/V)\to 0} (Z-1)V = B \quad (8)$$

This method is very sensitive to errors in density at low densities, so that the extrapolation can be extensive and the values obtained rather questionable. In like manner the third virial can be evaluated by graphically determining:

$$\lim_{(1/V)\to 0} (Z-1)V^2 - BV = C \quad (9)$$

This plot is very sensitive to the value of B and will blow up rather than extrapolate with negligible curvature if an erroneous value of B has been used. It is because of these difficulties that the experimental methods which screen out first-order effects may become more widely used.

Transport properties

Recent correlation efforts have shown that relationship between the nonequilibrium properties, *e.g.*, viscosity and thermal conductivity, and the equilibrium *P-V-T* property continues to gain support. On the basis of suggestions by Russian writers, Owens and Thodos (*8*) and others have made extensive use of the relationship between residual thermal conductivity and the density of a fluid to correlate data to a single curve. Eakin and Ellington (*3*) and Starling and Ellington (*2*) have shown that liquid, gas, and dense fluid viscosities can be correlated similarly. The dependence has been shown (*2*) to have fundamental basis in the modern molecular theory of fluids.

It is significant that these efforts yield continuity of states in the correlations. The correlations also show that for extensive ranges of conditions a single viscosity value results for a single density, whether that density represents a highly compressed gas, dense fluid, or a liquid at elevated temperature and low pressure. This has been shown to obtain for both pure components and mixtures (*9*). This situation is especially important in the extra emphasis that it places on the need for accurate prediction of densities of all fluid phases and preferably with a single relationship. Further confirmation of this need has been found because of the significant composition dependence of the correlation, both from the viscosity mixing rule standpoint and that of the density. In a case or two, erroneous sample analyses were detected through these sensitivities.

In recapitulation, great expansion in the uses of *P-V-T* information in the last decade, particularly in the calculations made possible by high speed computers, has resulted in greater need than ever for high quality *P-V-T*-composition data for all conditions of fluid existence. There is great need for improved equation of state representation of these data for the full range of conditions and for fundamental studies. Finally, increased accuracy is needed in both the basic data and the various repre-

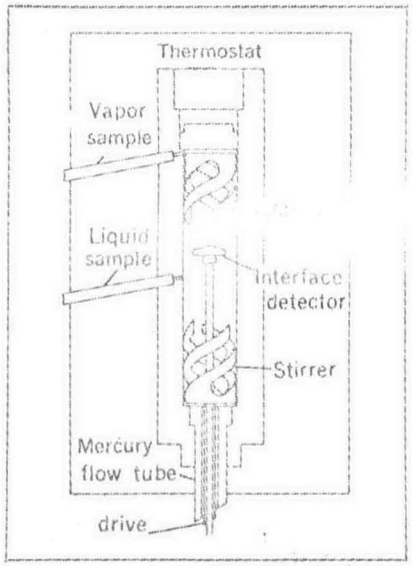

Figure 8. Sage and Lacey cell with liquid surface locator (26).

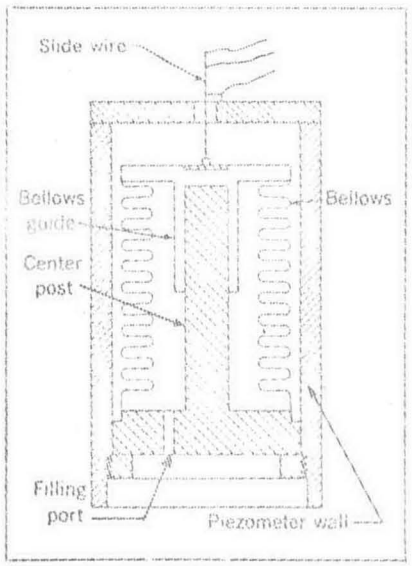

Figure 9. Schematic diagram of Bridgeman bellows cell (27).

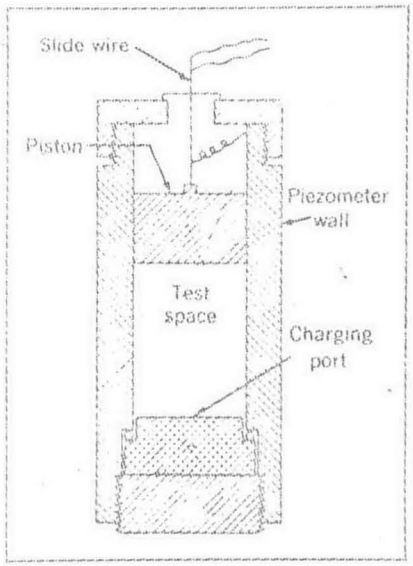

Figure 10. Schematic diagram of Bridgeman free piston cell (27).